Bull. Mater. Sci. (2019) 42:238
https://doi.org/10.1007/s12034-019-1926-x

Villari effect in silicone/FeGa composites

G RIESGO[1], L ELBAILE[2], J CARRIZO[2], G GARCÍA[2], R D CRESPO[2,*], M A GARCÍA[3], Y TORRES[4] and J A GARCÍA[2]

[1]Centro de Seguridad Marítima Integral Jovellanos, Camín del Centro de Salvamento no. 279, 33393 Gijón, Spain
[2]Departamento de Física de la Universidad de Oviedo, c/ Calvo Sotelo s/n, 33007 Oviedo, Spain
[3]Departamento de Ciencia de los Materiales, Universidad de Oviedo, c/ Independencia no. 13, 33004 Oviedo, Spain
[4]Departamento de Ingeniería y Ciencia de los Materiales y el Transporte, Universidad de Sevilla, 41092 Seville, Spain
*Author for correspondence (charo@uniovi.es)

MS received 23 January 2019; accepted 22 April 2019; published online 23 July 2019

Abstract. This paper presents the results of the Villari effect study in FeGa magnetorheological composites with very low stresses. The composites consist of a silicone matrix and Fe75Ga25 powder of size ranging from 50 to 100 μm. Two types of composites, one is with 45 wt% and the other one with 30 wt% of Fe75Ga25 powder have been manufactured. The Villari effect has been measured in both samples as-manufactured and in those in which a 1 T magnetic field has been applied after curing. The results indicate that the composites with an applied field of 1 T after curing show the greatest Villari signal even without any applied magnetic field. This fact allows a design of a low-cost force sensor and high performance. A simple model, based on the change in the cross-section of the composite, has been developed to explain the results obtained.

Keywords. Villari effect; magnetostrictive composites; FeGa powder.

1. Introduction

Magnetorheological elastomers (MR elastomers) are composites based on highly elastic polymeric matrices filled with magnetic micro- or nano-particles whose elastic properties depend on the applied magnetic field. Although the first report about the magnetorheological elastomer effect was reported in 1940 by Rabinow [1], it was in the 1990s, with the studies carried out by Jolly *et al* [2,3] when interest on the applications of these new materials was at its peak. Nowadays, there is a great interest in these composites because they present interesting properties for different applications in the biomedical field: e.g., to manufacture artificial muscles [4], in the control of drug delivery by the manufacture of active scaffolds [5], valveless micropumps [6] and hyperthermia, using composites with magnetite nanoparticles dispersed in a silicone matrix, which allow an increase in the temperature from 36 to 42°C [7]. Also, they are used in the automobile industry for applications in the vehicle seat vibration suspension [8] and civil engineering [9–11].

Basically, a MR elastomer consists of two or three basic components: an elastomeric matrix, magnetic particles and sometimes additives: silicone oil, glass powders, etc. By varying the polymeric matrix, particle size and concentration of magnetic particles [12–16], suitable composites can be obtained for mechanical, magnetic and electrical applications. MR elastomers can be classified into two groups: isotropic MR and anisotropic MR elastomers. In the first group, the composite is cured without any magnetic field and the magnetic particles are randomly distributed. Meanwhile, in those of the second group, the composite is cured under a magnetic field that produces an alignment of the particles. The mechanical and magnetic properties of composites vary on the magnetic particle distribution depending on the random or aligned distribution of the magnetic particles [17,18].

Another relevant characteristic of the MR elastomers is their high magnetostriction [19–23] that makes them excellent candidates to be used in stress and force sensors.

The Villari effect, also known as the inverse magnetomechanical effect, refers to the changes in magnetization of a magnetostrictive material when it is subjected to an applied stress. This effect is object of study given its applications, such as nondestructive evaluation and sensing [24–26].

In this paper, we present the results of the Villari effect in isotropic MR elastomers fabricated with a silicone matrix and Fe75Ga25 particles ranging from 50 to 100 μm obtained by mechanical milling from amorphous ribbons of the same composition obtained by a melt spinning process. Two types of samples have been manufactured, one is with 45 wt% of Fe75Ga25 powder and the other one with 30 wt%. These percentages have been chosen to obtain an appropriate magnetic signal to produce a deformation of the composites without a high increase in its rigidity. The Villari effect has been measured, with and without an applied field of 2 mT, in the as-manufactured samples and in samples subjected to an applied magnetic field of 1 T after curing.

An interesting result obtained in this work is that submitting the isotropic composites to a magnetic field of 1 T after cured,

produces a good response of the Villari effect without having to use a coil to magnetize the sample. A simple model based on the magnetic remanence of the composite and on changing the transverse cross-section of the sample under a tensile stress has been developed to explain this result. The model was tested in both the composites.

2. Experimental

2.1 *Starting materials*

High purity (99.9%) Fe and Ga metals were used as raw materials. Fe75Ga25 alloy ingots were prepared by induction melting under a vacuum atmosphere. From these ingots, ribbons of 2 mm wide and 60 μm thick were produced by planar flow casting in a vacuum atmosphere with a roll speed of 17.5 m s^{-1}. The chemical composition of the ribbons was determined by inductively coupled plasma.

Ribbons were manually cut and then cropped in a crusher (breaker) Fritsch Pulverisette P25 before being milled. This procedure allows the homogenization of ribbon sizes, reducing them to <1 mm. The milling was performed with a high-energy planetary ball-mill Retsch PM-400 (Retsch GmbH, Germany) in a 125 ml stainless steel vessel. Cropped ribbons and grinding media (10 mm diameter stainless steel ball) were loaded in a BPR 1:10 weight ratio with a rotation velocity of 200 rpm. The powder was divided by the coulter to obtain two different particle size distributions; one with a diameter ranging from 20 to 50 μm and the other one from 50 to 100 μm.

2.2 *Powder characterization*

The morphology of the powder was studied by using a scanning electron microscope (SEM) JEOL 6460LV. X-ray diffraction (XRD) patterns of the Fe75Ga25 powder were carried out in the Seifert XRD 3000TT diffractometer. The configuration of the equipment is Bragg–Brentano with Omega–Theta movement (detector–sample), with radiation being emitted by a thin focus Mo X-ray tube ($\lambda = 0.71075$ Å). The measurements were taken from 7 to 57° in steps of 0.04° at room temperature to determine the crystalline phases. The crystallite size and lattice strain of the powder during milling were determined by the Rietveld method using Topas 4.2 software.

2.3 *Fabrication of composites*

The powders with diameters between 50 and 100 μm have been used to fabricate two sets of composites using a silicone matrix (Silicone Ceys Ms-Tech). The composites were prepared by mixing the powders in a proportion of 30 and 45 wt% of Fe75Ga25 with silicone in the following way: all the components were mixed with a stirrer bar at room temperature and the mixture was put into a prism-shaped mould with dimensions of 50 × 30 mm and a thickness of 10 mm. The samples were cured without applying any magnetic field (isotropic composites). After manufacturing, the isotropic composites were subjected to an applied magnetic field of 1 T in the longitudinal direction of the sample magnetizing it in this direction.

2.4 *Composite characterization*

The magnetic characterization of the composites at room temperature was performed using a vibrating sample magnetometer (EV9-VSM 2.2 T).

The Young's modulus of the composite has been obtained from tensile stress–strain experiments and from the indentation test (P–h curves). The tensile stress–strain measurements were performed in a universal tester MTS400/M. The machine has a load cell of 2 kN and flat grips. The specimens were tested in tension with a gauge length, as defined by the hot zone, of 50 mm. A constant cross-head speed of 5 mm min^{-1} was employed to conduct the tension experiments along the length direction of the composite at a frequency of 10 Hz. P–h curves were performed with a Microtest device (MTR3/50-50/NI), at an applied load rate of 1 N min^{-1} and a holding time of 10 s. To perform the measurements, the samples were fixed to a steel cylinder. The surface of the samples was prepared using fine abrasive papers; the final polishing was performed with diamond particles in suspension and colloidal silica. At least five measurements were made for each type of material and test condition. The Young's modulus from the resulting load–penetration curves were evaluated using the Oliver and Pharr analysis [27–30].

The experimental system to measure the Villari effect is shown in figure 1. It consists of a direct power supply which provides an electrical current to a primary coil to magnetize the sample. This coil of 50 mm inner diameter consists of 360 turns of copper wire of 1 mm diameter and generates a maximum magnetic field of 2 mT A^{-1}. The Villari signal is obtained by means of a fluxmeter connected to the pickup coil that surrounds the sample, which is also connected to other identical secondary winding in series opposition. The pickup provides a signal proportional to B, and the secondary winding provides a signal proportional to $\mu_0 H_a$. Therefore, the fluxmeter provides a signal proportional to M. These secondary coils of 7 mm inner diameter consist of 20,000 turns of copper wire of 0.05 mm diameter.

To apply the tensile stress to the sample, one of its ends was attached to a fixed jaw and the other to a mobile, from which a weight holder was suspended. Various weights could be added to the holder by changing the applied stress.

The measurements of the Villari effect have been performed in a five loading/unloading cycles to ensure their repetitivities.

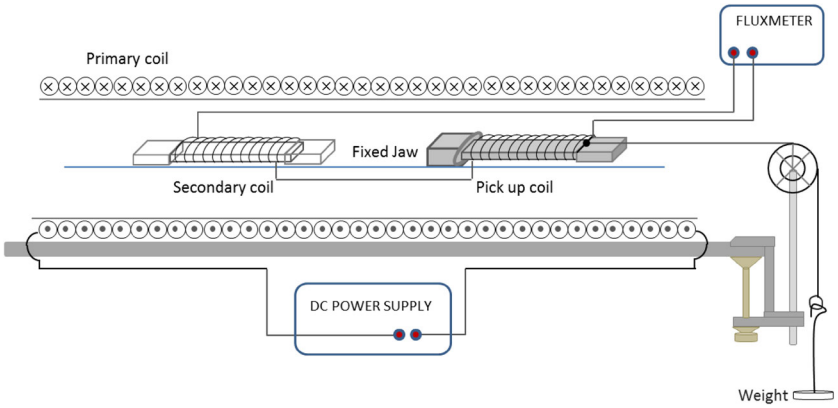

Figure 1. Experimental setup for measuring the Villari effect.

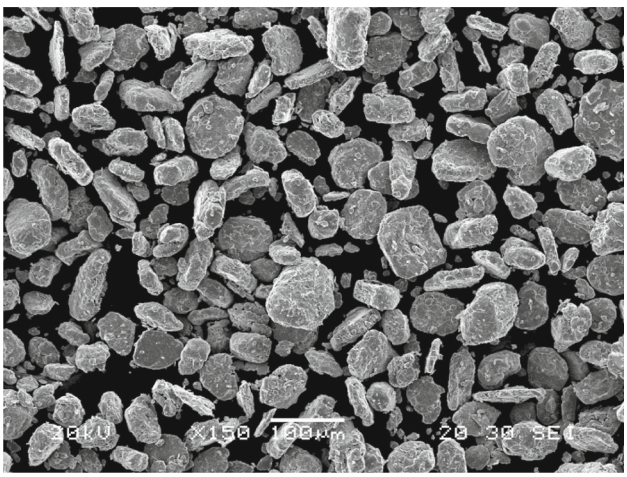

Figure 2. SEM image of the Fe75Ga25 particles.

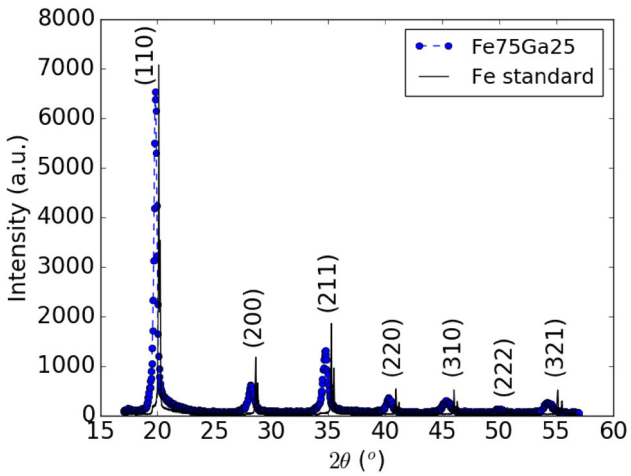

Figure 3. XRD patterns of Fe75Ga25 powder and a standard sample of Fe.

3. Results and discussion

A SEM micrograph of powder after 30 h milling is shown in figure 2. The XRD patterns of Fe75Ga25 powder as well as the XRD of a standard sample of Fe that allows us to determine the alignment error in a diffractometer are shown in figure 3. The reflections at 2θ: 19.8, 28.2, 34.7, 40.3, 45.3, 49.9 and 54.2° correspond to the phases (110), (200), (211), (220), (310), (222) and (321), respectively. As can be seen, the XRD patterns show that only peaks originating from the disordered BBC structure are observed. The introduction of Ga atoms into the cubic cell body-centred (BCC) Fe initiates an increase in cell size, which results in a shift of the Bragg peaks at low angles, while the grain size reduction due to grinding leads to a widening of the same.

From the microstructural parameters, the average size of the crystallite and average microdeformation have been determined according to the different directions of the reciprocal space; so the average size of the crystallite is 13 ± 5 nm, while the average microdeformation is $0.26 \pm 0.13\%$. The reduction in the grain size and an increase in microdeformation observed in reflections (200, 310) are indications of the presence of planar effects caused by the mechanical alloy to which the Fe75Ga25 powder has been subjected.

Four different samples have been studied and from now on we will refer to the composites as C30 and C40 correspond to the samples with 30 and 45% powder, respectively and C30F and C45F to the composites of the same percentage as the previous ones and subjected to a magnetic field of 1 T after curing.

Figure 4 shows the micrographs of C45 and C45F isotropic composites. As can be seen, no differences in powder distribution can be appreciated between both samples and confirm the isotropic distribution of the particles.

The magnetic hysteresis loops of the composites are shown in figure 5. As can be observed, the saturation magnetization of the C30 sample is smaller than that of C45 samples. This is due to its lower content of magnetic powder. In the inset of the same figure, an enlargement of the central part of hysteresis

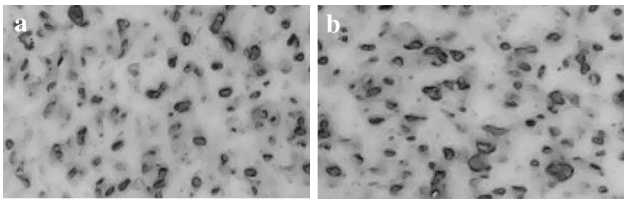

Figure 4. Images of the isotropic composites; (**a**) as-manufactured and (**b**) after submitting it to a magnetic field of 1 T.

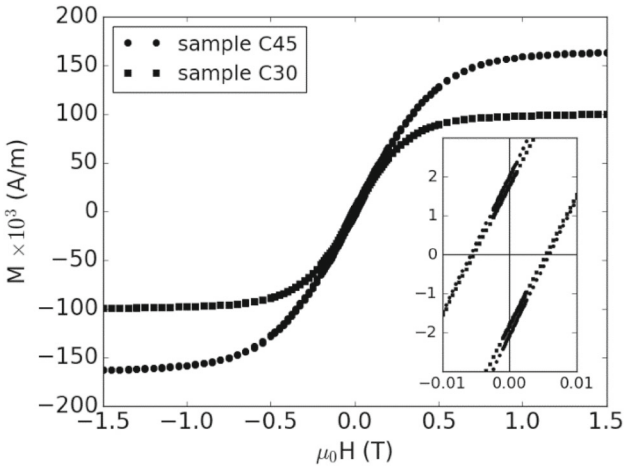

Figure 5. Hysteresis loops of the as-manufactured composites with 30 and 45 wt% Fe75Ga25 powders. In the inset, the central part of hysteresis loops is shown.

loops is shown and a remanence magnetization of 1800 ± 20 A m^{-1} for the C30 sample and 2000 ± 20 A m^{-1} for C45 sample can be appreciated.

Figure 6 shows the results of the Villari effect in the composites with 30 and 45 wt% Fe75Ga25 powder cured without any magnetic field and after subjecting them to an applied magnetic field of 1 T after curing. As expected, it can be seen that the Villari signal is greater in those samples with a higher percentage in magnetic particles and also we can observe that there is no hysteresis. Also, in the measurements performed with an applied field of 2 mT, the samples C30F and C45F present a greater Villari signal than their corresponding as manufactured ones, samples C30 and C45. In addition, a variation of the magnetic flux with tension has been measured without the application of any magnetic field in samples C30F and C45F.

The Villari effect in magnetorheological elastomers has been recently studied [31,32]. In these studies, the Villari signal obtained when a magnetic field is applied to the sample has been fitted to a second-order polynomial approximation.

In our samples, a Villari signal has been obtained without the need to apply any magnetic field to the sample. So, to explain these results, we propose a simple model based on the change in the cross-section of the composite when subjected to a tensile stress, which would explain the magnetic flux values obtained for the C30F and C45F samples when no magnetic field is applied.

In this way, taking into account the elastic properties of the studied composites and the narrow range of applied tensile stresses (ranging from 0.01 to 0.1 MPa), we assume the volume of the sample to be constant and therefore:

$$(l + \Delta l)s' = ls, \tag{1}$$

where l and Δl are the initial length and the length variation after deformation; s and s' are the cross-sections before and after straining, respectively. On the other hand, as well known, the relation between the tensile stress σ, the Young's modulus E and the strain ε can be written as:

$$\sigma = E\varepsilon. \tag{2}$$

From equations (1) and (2), we obtain after straining cross-section

$$s' = \frac{sE}{E + \sigma}. \tag{3}$$

On the other hand, considering that magnetic flux in the composite before and after straining are given by:

$$\Phi = \mu_0 MNs \quad \text{and} \quad \Phi' = \mu_0 M' N s', \tag{4}$$

where M and M' are the sample magnetizations before and after straining, N the number of turns of the pick-up coil and μ_0 the permeability of free space. If we assume that the composites present an initial magnetization and that ΔM is due to the low stress, we can write according to Brown [33]:

$$\Delta M = \beta\sigma^2, \tag{5}$$

where σ is the applied stress and β a constant. The composite magnetization after straining can be written as

$$M' = M + \beta\sigma^2. \tag{6}$$

Therefore, the change in magnetic flux resulting from the application of stress is given by:

$$\Delta\Phi = \mu_0 N\left(M's' - Ms\right) = \mu_0 Ns\left(\frac{\beta\sigma^2 E - M\sigma}{E + \sigma}\right). \tag{7}$$

To compare the predicted result by the model and the experimental data, the Young's modulus of the samples C30 and C45 have been measured.

Figure 7 shows the stress–strain curve obtained under elongation. Despite the lack of linearity that the curve presents, due to the small stress applied to the composites, a linear dependence between strain and stress can be assumed (inset

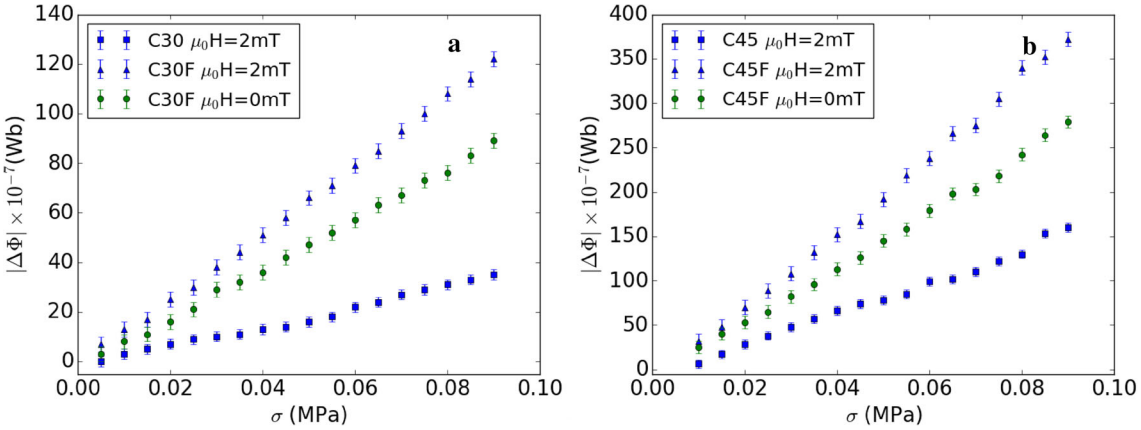

Figure 6. Magnetic flux as a function of applied stress in composites of Fe75Ga25 with (**a**) 30 wt% powder and (**b**) 45 wt% powder. For the C30 and C45 samples, the measurements have been carried out by applying a magnetic field of 2 mT; the C30F and C45F samples have been measured by applying a magnetic field of 2 mT and without any applied magnetic field.

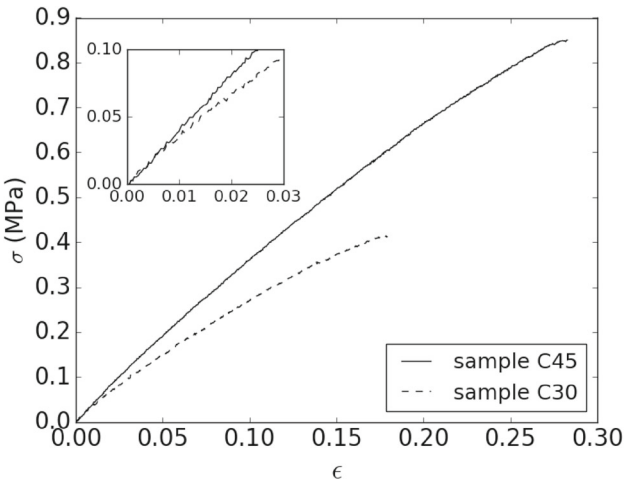

Figure 7. Stress–strain curves for composites with 30 and 45 wt% of Fe75Ga25. The inset shows an enlargement of curves in the stress range of the present work.

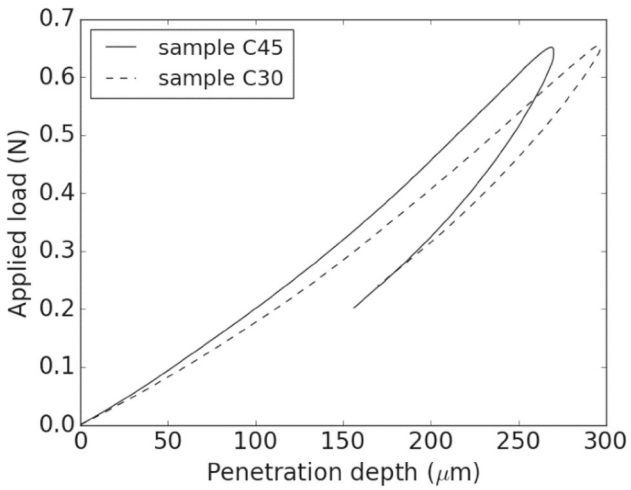

Figure 8. *P–h* curves for the as-manufactured C30 and C45 composites.

of figure 7). From these measurements, the Young's moduli obtained for the C30 and C45 composites are 3.3 ± 0.2 and 4.1 ± 0.3 MPa, respectively. The values obtained by microindentation are 2.72 ± 0.08 and 3.2 ± 0.1 MPa, respectively, and the corresponding *P–h* curves are shown in figure 8.

To check the model, the measurements without any applied magnetic field, for the mentioned C30F and C45F samples in figure 6, have been fitted using the function:

$$\Delta\Phi = \frac{a\sigma^2 - b\sigma}{E + \sigma}, \tag{8}$$

where a and b are parameters, according to the model, b represents the initial magnetic flux of the sample without applied stress. Figure 9 shows the good agreement between experimental data and fitting.

The initial magnetic flux measured by the induction method and the values of the parameter b obtained from the fitting for both samples are shown in table 1.

To check the model with the Villari effect measurements performed with a magnetic field of 2 mT, it has been assumed that this low field increases the initial magnetization of the samples previous to the application of tensile stress. Therefore, it is possible to obtain the different states of magnetization for the samples under this field from the experimental data fitting. Figure 10 shows the fittings obtained for the Villari signal of the C30 and C30F composites with a magnetic field of 2 mT. Again, a good agreement between experimental data and fitting can be appreciated. The estimated initial magnetization of the C30F and C45F composites obtained from

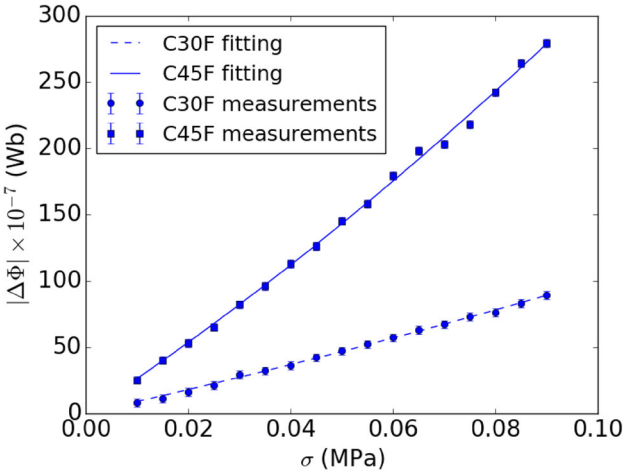

Figure 9. Magnetic flux, without any magnetic field, as a function of applied stress and its fitting of C30F and C45F composites.

Table 1. Results of the initial magnetic flux for the as-manufactured sample after submitting it to a magnetic field of 1 T after cured.

	$\mu_0 N s M_0 \times 10^{-4}$ (Wb)	
Sample	Fitting	Measures
C30F	2.95 ± 0.06	3.8 ± 0.1
C45F	8.2 ± 0.2	7.7 ± 0.1

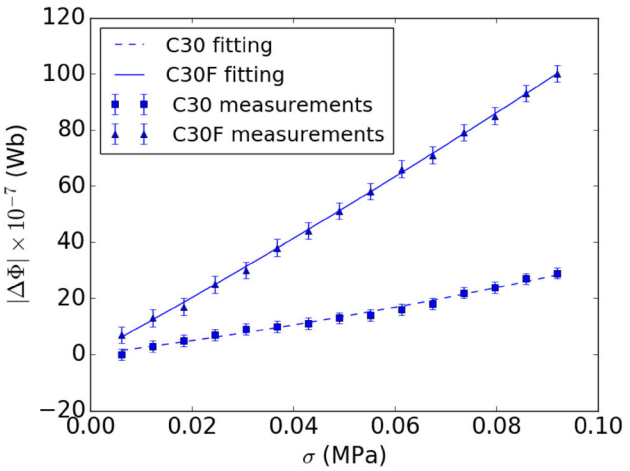

Figure 10. Magnetic flux with a magnetic field of 2 mT as a function of applied stress and its fitting of 30 wt% of Fe75Ga25 composites.

the measurement fittings is shown in table 2. As expected, due to its low percent of magnetic particles, the C30F sample has a smaller initial magnetization than the C45F sample. On the other hand, the model predicts an initial magnetization for both samples in the absence of an applied magnetic field and applying a magnetic field of 2 mT in the measurement of the Villari effect, the magnetization of the previously magnetized samples is increased, which produces an increase in the measured Villari signal.

Table 2. Initial magnetization obtained from the fitting of the magnetic field as a function of stress for C30F and C45F composites.

	Initial magnetization (A m^{-1})	
Sample	$\mu_0 H = 0$ mT	$\mu_0 H = 2$ mT
C30F	734 ± 15	808 ± 9
C45F	1660 ± 40	2200 ± 50

The model developed in this work describes the results obtained in premagnetized samples in the very low-stress regime and considering the Young modulus and Poisson coefficient constant.

4. Conclusion

In this paper, the Villari effect in silicone FeGa composites has been studied. The results indicate, on the one hand, that the samples with an applied field of 1 T after curing and submitted to an applied magnetic field of 2 mT to measure the Villari effect show a greater signal than those as manufactured; on the other hand, the samples with an applied field of 1 T after curing give an outstanding Villari signal without any applied field. Taking into account that the samples are saturated after being submitted to a magnetic field of 1 T (figure 5), this behaviour is due to the initial remanence magnetization that samples present.

A simple model, based on the change of the cross-section of the composite has been developed to explain the results obtained.

To check the model, the measured data for the samples with an applied field of 1 T after curing have been fitted to $\Delta\Phi = (a\sigma^2 - b\sigma)/(E + \sigma)$, with a and b as parameters; where b means the initial magnetic flux of the sample without stress. As can be seen in figure 9, there is a good fitting between the experimental data and the measurements.

Obtaining a Villari signal in these samples without applying a magnetic field, makes these materials very promising for use in force and deformation sensors.

Acknowledgements

This work was supported in part by the Principality of Asturias governments under grant GRUPIN 14-037. We are grateful to Dr D Martínez, in charge of Magnetic Measurements and the X-ray Diffraction of the Scientific Services of the University of Oviedo.

References

[1] Rabinow J 1948 *Natl. Bureau Stand. Tech. News Bull.* **32** 54
[2] Jolly M R, Carlson J D and Muñoz B C 1996 *Smart Mater. Struct.* **5** 607
[3] Jolly M R, Carlson J D, Muñoz B C and Bullions T A 1996 *J. Intell. Mater. Syst. Struct.* **7** 613
[4] Nguyen V Q, Ahmed A S and Ramanujan R V 2012 *Adv. Mater.* **24** 4041
[5] Zhao X, Kim J, Cezar Ch A, Huebsch N, Lee K, Bouhadir K *et al* 2011 *Proc. Natl. Acad. Sci. USA* **108** 67
[6] Zhou X and Amirouche F 2011 *Micromachines (Basel)* **2** 345
[7] Pirmoradi F N, Jackson J K, Burt H M and Chiao M 2011 *Lab. Chip* **11** 3072
[8] Li W, Zhang X and Du H 2012 *J. Intell. Mater. Syst. Struct.* **23** 1041
[9] Eem S H, Jung H J and Koo J H 2011 *IEEE Trans. Magn.* **47** 2901
[10] Li Y, Li J, Li W and Du H 2014 *Smart. Mater. Struct.* **23** 123001
[11] Ubaidillah, Sutrisno J, Purwanto A and Mazlan S 2015 *Adv. Eng. Mater.* **17** 563
[12] Abramchuk S, Kramarenko E, Stepanov G, Nikitin L V, Filipcsei G, Khokhlov A R *et al* 2007 *Polym. Adv. Technol.* **18** 883
[13] Ubaidillah, Imaddudin F, Li Y, Mazlan S A, Sutrisno J, Koga T *et al* 2016 *Smart. Mater. Struct.* **25** 115002
[14] Guskos N, Typek J, Padyak B V, Gorelenko Y K, Pelech I, Narkiewicz U *et al* 2010 *J. Non-Cryst. Solids* **356** 1893
[15] Siegried P, Koo J-H and Pechan M 2014 *Polym. Test.* **37** 6
[16] Makarova L A, Alekhina Y A, Rusakova T S and Perov N S 2016 *Phys. Procedia.* **82** 38
[17] Guan X, Dong X and Ou J 2008 *J. Magn. Magn. Mater.* **320** 158
[18] Kiseleva T Y, Zholudev S I, Il'inykh I A and Novakova A A 2013 *Tech. Phys. Lett.* **39** 1109
[19] Ginder J M, Clark S M, Schlotter W F and Nichols M E 2002 *Int. J. Mod. Phys. B* **16** 2412
[20] Riesgo G, Carrizo J, Elbaile L, Crespo R D, Sepúlveda R and García J A 2017 *Mater. Sci. Eng. B* **215** 56
[21] Zhao R, Wang B, Cao S, Huang W, Lu Q and Yan J 2018 *J. Magn.* **23** 280
[22] Narita F and Fox M 2018 *Adv. Eng. Mater.* **20** 1700743
[23] Yoffe A, Kaniel H and Shilo D 2017 *Funct. Mater. Lett.* **10** 1750060
[24] Dapino M J, Smith R C, Calkins F T and Flatau A B 2002 *J. Intell. Mater. Syst. Struct.* **13** 737
[25] Wang H B and Feng Z H 2013 *IEEE Trans. Magn.* **49** 1327
[26] Al-Hajjeh A, Lynch E, Law Ch T and El-Hajjar R 2016 *IEEE Magn. Lett.* **7** 6502804
[27] Oliver W C and Pharr G M 2004 *J. Mater. Res.* **19** 3
[28] Harding D S, Olive W C, Pharr G M, Baker S P, Børgesen P, Townsend P H *et al* 1995 *V. MRS Sympos. Proc.* **356**
[29] Oliver W C and Pharr G M 1992 *J. Mater. Res.* **7** 1564
[30] Sneddon I N 1965 *Int. J. Eng. Sci.* **3** 47
[31] Sebald G, Nakano M, Lallart M, Tian T, Diguet G and Cavaillé J 2017 *Sci. Technol. Adv. Mater.* **18** 766
[32] Diguet G, Sebald G, Nakano M, Lallart M and Cavillé J 2019 *J. Magn. Magn. Mater.* **481** 39
[33] Brown W F 1949 *Phys. Rev.* **75** 147